16 March 2001

ELSEVIER

Chemical Physics Letters 336 (2001) 187–195

CHEMICAL PHYSICS LETTERS

www.elsevier.nl/locate/cplett

Nodal surface approximations to the P, G, D and I-WP triply periodic minimal surfaces

Paul J.F. Gandy [a], Sonny Bardhan [a], Alan L. Mackay [b], Jacek Klinowski [a,*]

[a] *Department of Chemistry, University of Cambridge, Lensfield Road, Cambridge CB2 1EW, UK*
[b] *Department of Crystallography, Birkbeck College, University of London, Malet Street, London WC1E 7HX, UK*

Received 8 August 2000

Abstract

The cubic P, G, D and I-WP triply periodic minimal surfaces (TPMS) may be closely approximated using periodic nodal surfaces (PNS) with few Fourier terms, thus enabling easy generation of TPMS for use in various chemical and physical applications. The accuracy of such approximations is quantitatively discussed and represented visually using a colour coding. © 2001 Elsevier Science B.V. All rights reserved.

1. Introduction

A minimal surface is a surface for which the mean curvature $H = (k_1 + k_2)/2$ is zero at every point, where k_1 and k_2 are the principal curvatures in two mutually orthogonal planes [1]. The divergence of the unit normal vector is thus zero everywhere. The Gaussian curvature is defined as $K = k_1 k_2$. A triply periodic minimal surface (TPMS) is infinite and periodic in three independent directions. TPMS are omnipresent in the natural and man-made worlds, providing a concise description of many seemingly unrelated structures [2]. They are of interest not only to the structural chemist, but also to the biologist [3], structural engineer and the materials scientist [4]. Considering the cubic TPMS, the structure of the zeolite analcime is described by the G surface [5]; the P surface occurs in etioplasts and in sea urchin spines [3]; and the D surface is found in glyceryl mono-oleate/water mixtures [6]. However, TPMS have so far been identified in real structures by visual inspection. In order to be able to compare real structures (for example, those stored in the Cambridge Crystallographic Database) with TPMS, it is necessary to be able to generate the precise surface coordinates.

TPMS are built of fundamental units spanning the asymmetric domain in a given crystallographic symmetry group. Repetition of the unit by rotation about a twofold axis along its perimeter, or by mirror planes, gives rise to an infinite non-self-intersecting surface. Some TPMS divide space into two congruent regions which may (the G surface) or may not (the P and D surfaces) be mirror images of one another and are known as 'balanced' surfaces. Unbalanced surfaces, such as the I-WP surface, divide space into labyrinths of unequal volumes.

There are several ways of arriving at the coordinates of TPMS. The Enneper–Weierstrass representation [7] gives the coordinates of a minimal surface as

* Corresponding author. Fax: +44-01223-336362.
E-mail address: jk18@cam.ac.uk (J. Klinowski).

0009-2614/01/$ - see front matter
PII: S0009-2614(00)01418-4

$$x = \mathrm{Re}\int_{\omega_0}^{\omega} \mathrm{e}^{\mathrm{i}\theta}(1-\tau^2)R(\tau)\,\mathrm{d}\tau,$$

$$y = \mathrm{Re}\int_{\omega_0}^{\omega} \mathrm{e}^{\mathrm{i}\theta}\mathrm{i}(1+\tau^2)R(\tau)\,\mathrm{d}\tau, \qquad (1)$$

$$z = \mathrm{Re}\int_{\omega_0}^{\omega} \mathrm{e}^{\mathrm{i}\theta}2\tau R(\tau)\,\mathrm{d}\tau,$$

where $\mathrm{i}^2 = -1$ and $\tau = \tau_a + \mathrm{i}\tau_b$, associating with function $R(\tau)$ (the Weierstrass function) a surface which is guaranteed to be minimal; θ is known as the Bonnet angle. The Cartesian coordinates of any point are expressed as the real parts (Re) of contour integrals, evaluated in the complex plane from some fixed point ω_0 to a variable point ω. The coordinates of a minimal surface are determined by evaluating the integrals of its Weierstrass function. Unfortunately, the function is known only for several TPMS. It can be constructed if there exists a surface patch from which the entire surface can be generated by reflection or rotation about the patch boundary [8–13], but not every surface has this property. Analytical solutions using this method have been given for the P, D, G and I-WP surfaces in terms of elliptic [14–16] and hypergeometric [17] functions.

TPMS can also be constructed using conjugate surface methods, by converting the free boundary problem to the Plateau problem using the Bonnet transformation. The method has been applied to prove the existence theorems of conjectured TPMS [18] and to generate new surfaces, but is limited to surfaces of low genus.

The Surface Evolver, a computer program devised by Brakke [19], enables the numerical generation of minimal surfaces. The coordinates of a surface of mean curvature H_0 are calculated by determining the zero levels of the energy $\int (H - H_0)^2\,\mathrm{d}S$ using a finite element method. The program also indicates whether or not the surface in question would be physically stable.

1.1. Periodic nodal surfaces

TPMS, as well as other periodic surfaces, such as the Fermi [20] and equipotential [21] surfaces, can be approximated by the periodic nodal surface (PNS) of a sum defined in terms of the Fourier series [22,23]

$$\Psi(\mathbf{r}) = \sum_{\mathbf{k}} F(\mathbf{k})\cos[2\pi\mathbf{k}\cdot\mathbf{r} - \alpha(\mathbf{k})] = 0, \qquad (2)$$

where $\mathbf{k}$ are the reciprocal lattice vectors for a given lattice, $\alpha(\mathbf{k})$ is a phase shift, and the structure factor $F(\mathbf{k})$ is an amplitude associated with a given $\mathbf{k}$-vector.

Von Schnering and Nesper reported that the topology of the TPMS is satisfactorily reproduced by truncating the series (2) to the leading term, giving the following nodal approximations of the P, D, G and I-WP surfaces [21]

$$\cos X + \cos Y + \cos Z = 0, \qquad (3a)$$

$$\cos X \cos Y \cos Z - \sin X \sin Y \sin Z = 0, \qquad (3b)$$

$$\sin X \cos Y + \sin Z \cos X + \sin Y \cos Z = 0, \qquad (3c)$$

$$2(\cos X \cos Y + \cos Z \cos X + \cos Y \cos Z) - (\cos 2X + \cos 2Y + \cos 2Z) = 0, \qquad (3d)$$

where $X = 2\pi x$, $Y = 2\pi y$ and $Z = 2\pi z$ (Tables 1–4). The mean and Gaussian curvatures are given in terms of the unit normal vector $\mathbf{n}$ as [24]

$$H = \nabla\cdot\mathbf{n}, \qquad (4)$$

$$2K = \mathbf{n}\cdot\nabla^2\mathbf{n} + [\nabla\cdot\mathbf{n}]^2 + [\nabla\times\mathbf{n}]^2, \qquad (5)$$

where $\mathbf{n} = \nabla\Psi(\mathbf{r})/|\nabla\Psi(\mathbf{r})|$ and $\nabla = \mathbf{i}\partial/\partial x + \mathbf{j}\partial/\partial y + \mathbf{k}\partial/\partial z$.

Table 1
Parameters used in the nodal approximation to the P surface

$$\{hkl\} = \cos(hx)[\cos(ky)\cos(lz) + \cos(ly)\cos(kz)] + \cos(hy)[\cos(kz)\cos(lx) + \cos(lz)\cos(kx)] + \cos(hz)[\cos(kx)\cos(ly) + \cos(lx)\cos(ky)]$$

h	k	l	Coefficient
Fitting 5 terms			
1	0	0	1
1	1	1	−0.00956335
2	1	0	0.00959441
3	0	0	−0.0181364
2	2	1	−0.0292538
Fitting 2 terms			
1	0	0	1
1	1	1	−0.150763

Table 2
Parameters used in the nodal approximation to the D surface

$$\begin{aligned}\{h\,k\,l\} = {} & \cos\left(lz-\tfrac{k}{4}+\tfrac{h}{4}\right)\left(\cos\left(hx+\tfrac{l}{4}-\tfrac{k}{4}\right)\cos\left(ky+\tfrac{h}{4}-\tfrac{l}{4}\right)+\cos\left(hy+\tfrac{l}{4}-\tfrac{k}{4}\right)\cos\left(kx+\tfrac{h}{4}-\tfrac{l}{4}\right)\right)\\ & +\cos\left(lx-\tfrac{k}{4}+\tfrac{h}{4}\right)\left(\cos\left(hy+\tfrac{l}{4}-\tfrac{k}{4}\right)\cos\left(kz+\tfrac{h}{4}-\tfrac{l}{4}\right)+\cos\left(hz+\tfrac{l}{4}-\tfrac{k}{4}\right)\cos\left(ky+\tfrac{h}{4}-\tfrac{l}{4}\right)\right)\\ & +\cos\left(ly-\tfrac{k}{4}+\tfrac{h}{4}\right)\left(\cos\left(hz+\tfrac{l}{4}-\tfrac{k}{4}\right)\cos\left(kx+\tfrac{h}{4}-\tfrac{l}{4}\right)+\cos\left(hx+\tfrac{l}{4}-\tfrac{k}{4}\right)\cos\left(kz+\tfrac{h}{4}-\tfrac{l}{4}\right)\right)\\ & +\sin\left(lz-\tfrac{k}{4}+\tfrac{h}{4}\right)\left(\sin\left(hx+\tfrac{l}{4}-\tfrac{k}{4}\right)\sin\left(ky+\tfrac{h}{4}-\tfrac{l}{4}\right)+\sin\left(hy+\tfrac{l}{4}-\tfrac{k}{4}\right)\sin\left(kx+\tfrac{h}{4}-\tfrac{l}{4}\right)\right)\\ & +\sin\left(lx-\tfrac{k}{4}+\tfrac{h}{4}\right)\left(\sin\left(hy+\tfrac{l}{4}-\tfrac{k}{4}\right)\sin\left(kz+\tfrac{h}{4}-\tfrac{l}{4}\right)+\sin\left(hz+\tfrac{l}{4}-\tfrac{k}{4}\right)\sin\left(ky+\tfrac{h}{4}-\tfrac{l}{4}\right)\right)\\ & +\sin\left(ly-\tfrac{k}{4}+\tfrac{h}{4}\right)\left(\sin\left(hz+\tfrac{l}{4}-\tfrac{k}{4}\right)\sin\left(kx+\tfrac{h}{4}-\tfrac{l}{4}\right)+\sin\left(hx+\tfrac{l}{4}-\tfrac{k}{4}\right)\sin\left(kz+\tfrac{h}{4}-\tfrac{l}{4}\right)\right)\end{aligned}$$

h	k	l	Coefficient
1	1	1	1
3	3	1	0.0235559
5	1	1	0.00619501

Table 3
Parameters used in the nodal approximation to the G surface

$$\begin{aligned}\{h\,k\,l\} = {} & \cos\left(\tfrac{h+k+l}{4}\right)\left(\begin{array}{l}\left(\begin{array}{l}\cos\left(hx+\tfrac{l}{4}\right)\cos\left(ky+\tfrac{h}{4}\right)\cos\left(lz+\tfrac{k}{4}\right)+\cos\left(kx+\tfrac{h}{4}\right)\cos\left(ly+\tfrac{k}{4}\right)\cos\left(hz+\tfrac{l}{4}\right)\\ +\cos\left(lx+\tfrac{k}{4}\right)\cos\left(hy+\tfrac{l}{4}\right)\cos\left(kz+\tfrac{h}{4}\right)\end{array}\right)\\ +\cos\left(\tfrac{h+k+l}{4}\right)\left(\begin{array}{l}\cos\left(kx+\tfrac{l}{4}\right)\cos\left(hy+\tfrac{k}{4}\right)\cos\left(lz+\tfrac{h}{4}\right)+\cos\left(lx+\tfrac{h}{4}\right)\cos\left(ky+\tfrac{l}{4}\right)\cos\left(hz+\tfrac{k}{4}\right)\\ +\cos\left(hx+\tfrac{k}{4}\right)\cos\left(ly+\tfrac{h}{4}\right)\cos\left(kz+\tfrac{l}{4}\right)\end{array}\right)\end{array}\right)\\ & +\cos\left(\tfrac{h+k+l}{4}\right)\left(\begin{array}{l}\left(\begin{array}{l}\sin\left(hx+\tfrac{l}{4}\right)\sin\left(ky+\tfrac{h}{4}\right)\sin\left(lz+\tfrac{k}{4}\right)+\sin\left(kx+\tfrac{h}{4}\right)\sin\left(ly+\tfrac{k}{4}\right)\sin\left(hz+\tfrac{l}{4}\right)\\ +\sin\left(lx+\tfrac{k}{4}\right)\sin\left(hy+\tfrac{l}{4}\right)\sin\left(kz+\tfrac{h}{4}\right)\end{array}\right)\\ +\sin\left(\tfrac{h+k+l}{4}\right)\left(\begin{array}{l}\sin\left(kx+\tfrac{l}{4}\right)\sin\left(hy+\tfrac{k}{4}\right)\sin\left(lz+\tfrac{h}{4}\right)+\sin\left(lx+\tfrac{h}{4}\right)\sin\left(ky+\tfrac{l}{4}\right)\sin\left(hz+\tfrac{k}{4}\right)\\ +\sin\left(hx+\tfrac{k}{4}\right)\sin\left(ly+\tfrac{h}{4}\right)\sin\left(kz+\tfrac{l}{4}\right)\end{array}\right)\end{array}\right)\end{aligned}$$

h	k	l	Coefficient
1	1	0	1
2	2	2	−0.00382452
4	1	1	−0.000878436
3	3	0	0.00225091

Table 4
Parameters used in the nodal approximation to the I-WP surface

$$\{h\,k\,l\} = \cos^2\left(\frac{h+k+l}{4}\right)\left(\begin{array}{l}\cos(hx)[\cos(ky)\cos(lz)+\cos(ly)\cos(kz)]\\ +\cos(hy)[\cos(kz)\cos(lx)+\cos(lz)\cos(kx)]\\ +\cos(hz)[\cos(kx)\cos(ly)+\cos(lx)\cos(ky)]\end{array}\right)$$

Constant $a_0 = 0.0136536$

h	k	l	Coefficient
1	1	0	1
0	0	0	0.0819216
2	0	0	−0.107393
2	1	1	0.0517241
2	2	0	0.0555748
3	1	0	−0.0163199
2	2	2	−0.00705269
3	2	1	0.00476839

1.2. Generation of nodal surfaces

Although the 'leading-term-only' PNS are neither minimal nor constant-mean-curvature surfaces [25,26], they have been used as approximants for such surfaces [26–28]. Brenner et al. [29] have proposed the use of PNS to facilitate crystal structure solution from X-ray powder diffraction data. Their procedure constructs a PNS structure envelope using just a few low-index reflections, and has important implications for direct-space methods of structure determination. Framework atoms in 14 zeolites were found to lie on one side of the calculated curved surface.

The first-order approximation for the P, D, G and I-WP surfaces [21] used the {1 0 0} PNS in space group $Pm\bar{3}m$, {1 1 1} in space group $Fd\bar{3}m$ (origin $\bar{3}m$ or $\bar{4}3m$), {1 1 0} in space groups $I4_132$ and {1 1 0}in space group $Im\bar{3}m$ (phase angle $\alpha = 0$), respectively. The structure factor was calculated from

$$\sum_{h,k,l} \cos[2\pi(hx + ky + lz) + \alpha_{hkl}] = 0, \tag{6}$$

considering only one or two $\{h\,k\,l\}$ planes for each space group. We note that none of the resulting surfaces was actually shown and the quality of the nodal approximation was not quantitatively considered.

The space groups used in [21] are actually subgroups of the full generating space groups: $Im\bar{3}m$ (No. 229) (for the P surface), $Pn\bar{3}m$ (No. 224) (D surface), $Ia\bar{3}d$ (No. 230) (G surface) and $Im\bar{3}m$ (No. 229) (I-WP surface). TPMS where the two sides are of different colours (as for the D surface), may need the use of a full group and/or a different unit cell.

The quality of the approximation of a periodic surface by nodal surfaces depends on the number of terms in the Fourier series. We shall describe an easy and accurate way of approximating cubic TPMS by PNS. We have taken into account a larger number of Fourier terms, and calculated the (x, y, z) coordinates using Mathematica [30], by summing (6) over a set of $\{h\,k\,l\}$ planes appropriate for each space group [31–34]. Periodic density distributions are represented as the sums of three-dimensional Fourier series, with the terms $\cos[2\pi(hx + ky + lz)]$ and $\sin[2\pi(hx + ky + lz)]$ corresponding to centrosymmetric and antisymmetric waves, respectively. The position of a density point in the unit cell is (x, y, z), and the direction of the wave normal is $\{h\,k\,l\}$. For example, in the space group $Im\bar{3}m$, every scattering point is repeated by the symmetry elements to give a set of 48 waves, which can be consolidated into a single formula involving the general expressions for A and B, the centro-symmetric and the anti-symmetric components [31–34]. The value of B depends on the choice of origin of the unit cell. For an origin coinciding with the centre of symmetry, $B = 0$, but if, as is often convenient, we choose another origin, B is related to A by a phase shift. We therefore chose unit cell origin coincident with the centre of symmetry.

To represent a TPMS as the nodal surface, we first generate the coordinates of a given surface using the exact analytical expressions [14–17]. We next select the general structure factor expression for A for the appropriate space group, and set up an equation

$$f_0(x, y, z) + a_1 f_1(x, y, z) + a_2 f_2(x, y, z) + a_3 f_3(x, y, z) + \cdots + a_n f_n(x, y, z) = 0, \tag{7}$$

where $f_i(x, y, z)$ are the structure factor expressions for the set of planes considered, and the a_i are constant coefficients. The next step is to find a set of coefficients a_i which best fit the exact TPMS coordinates. The coefficient of the leading term, $f_0(x, y, z)$, in (7) is set to 1. The I-WP surface is unbalanced, and it is necessary to add a constant term, a_0, to (7). When fitting Fourier terms it is essential to use the Singular Value Decomposition (SVD) procedure rather than the Pseudo Inverse method, with a suitable tolerance to ensure stability [35].

The choice of the most suitable leading term was initially made intuitively or by trial and error [21]. In general, it is helpful to consider separately the indices {1 0 0}, {1 1 0}, {1 1 1}, etc., for the main space groups concerned and see whether the general shape of the desired TPMS is reproduced.

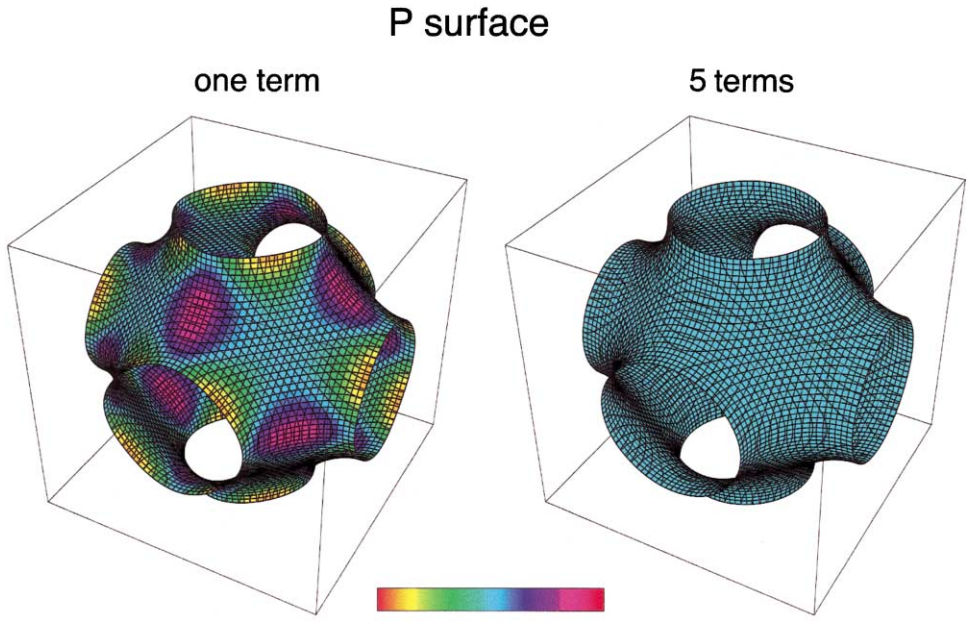

Fig. 1. Left: Colouring of the {1 0 0} nodal surface approximation to the P surface in the space group $Pm\bar{3}m$ according to the mean curvature (the value of $\nabla \cdot \mathbf{n}$) calculated at the centre of mass of each tessellating polygon. Right: Colouring of the nodal surface approximation to the P surface (Table 1). The light blue colour at the centre of the colour scale corresponds to zero mean curvature. The left-hand side has been assigned the numerical value 0, progressing to the value 1 as we move to the right-hand side. The colouring is cyclical so that 0 and 1 are of the same colour.

Trial nodal surfaces were plotted as tessellating polygons. The divergence of the unit vector normal to each polygon at its centre of gravity was calculated and represented visually by assigning a colour to the polygon (Figs. 1–4). Colours of the visible spectrum were assigned numerical values from 0 to 1 cyclically, so that 0.5 (light blue) corresponds to a minimal surface (i.e., to zero divergence). Thus, the colour assigned the numerical value of 0.2 represents $\nabla \cdot \mathbf{n} = -0.3$. The quality of each approximation can therefore be visualised. A quantitative assessment of the quality of the approximation was given by the value of $\sqrt{\langle(\nabla \cdot n)^2\rangle}$ at the centre of gravity. Clearly, the accuracy of the approximation increases with the number of polygons used to sample the surface.

1.3. Results and discussion

The leading-term-only nodal approximations to TPMS are shown on the left-hand side of Figs. 1–4 and the numerical results are listed in Table 5. It is clear that the general topology of all four TPMS is very well reproduced. The PNS approximating the D and G surfaces (Figs. 2 and 3) are very nearly minimal (see the rms values in Table 5) and can be used in practical applications (such as modelling of diffusion or the catalytic activity of the molecular sieves in which they occur) without further refinement. However, the PNS approximating the P surface (Fig. 1) contains patches, coinciding with areas of the highest Gaussian curvature, where the surface deviates considerably from minimal, and the approximation to the IW-P surface (Fig. 4 and Table 5) is generally unsatisfactory.

The leading-term-only approximations were refined by adding further terms whose zeros coincide with the symmetry of the surface, together with appropriate coefficients [26]. The structure factor expressions used are given in Tables 1–4. Symmetry simplifies the procedure. Thus the G and I-WP surfaces are body-centred cubic, so expansion terms are those for which the sum

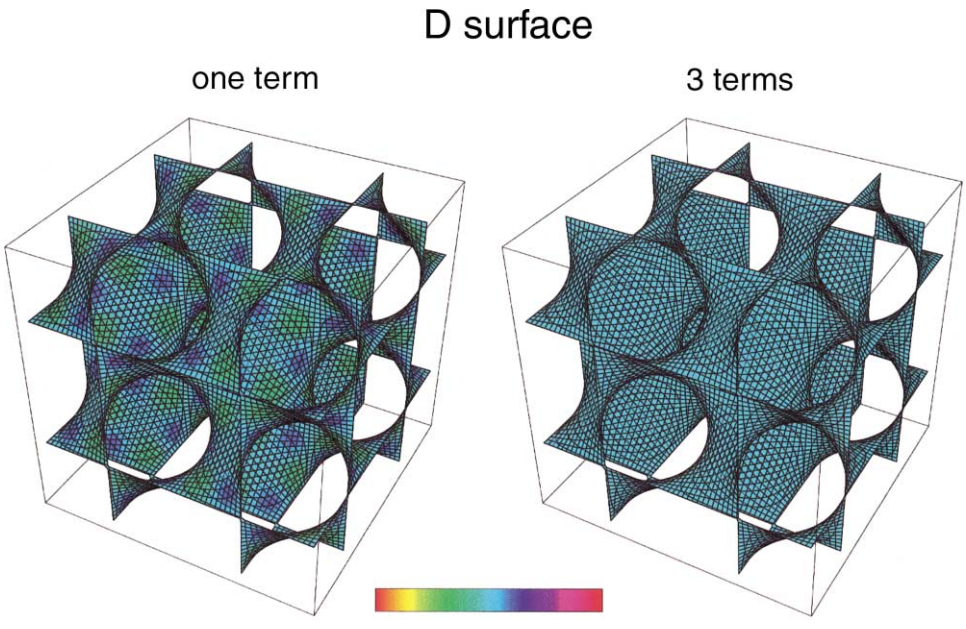

Fig. 2. Left: Colouring of the {1 1 1} nodal surface approximation to the D surface in the space group $Fd\bar{3}m$ according to the mean curvature calculated at the centre of mass of each tessellating polygon. Right: Colouring of the nodal surface approximation to the D surface (Table 2).

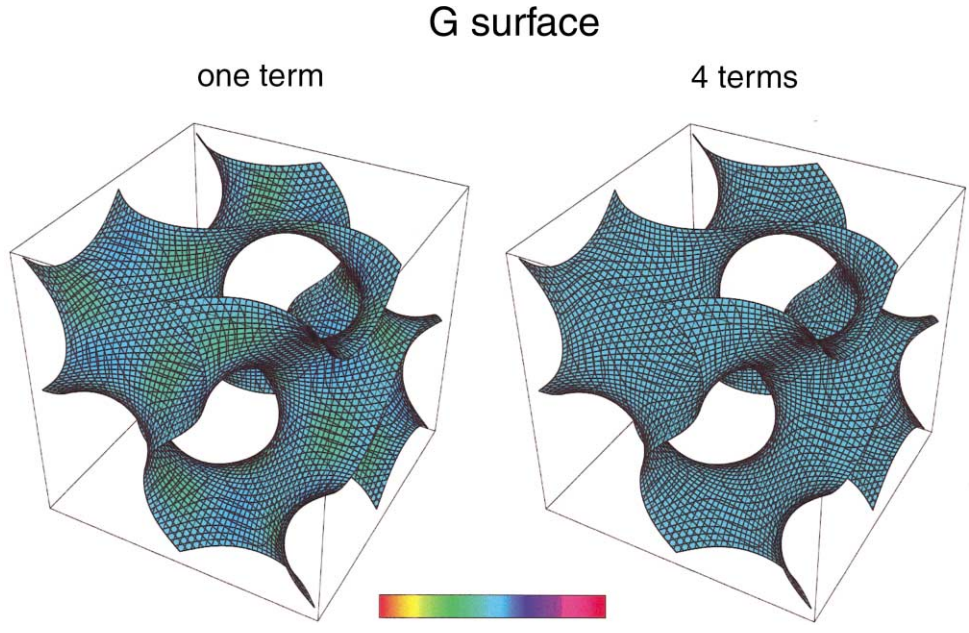

Fig. 3. Left: Colouring of the {1 1 0} nodal surface approximation to the G surface in the space group $I4_132$ according to the mean curvature calculated at the centre of mass of each tessellating polygon. Right: Colouring of the nodal surface approximation to the G surface (Table 3).

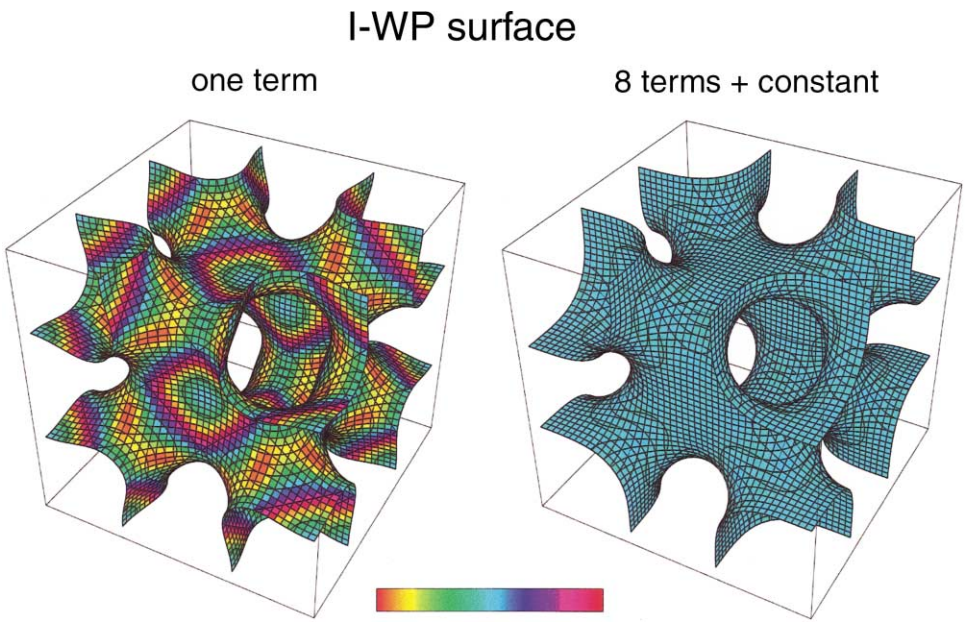

Fig. 4. Left: Colouring of the {1 1 0} nodal surface approximation to the I-WP surface in the space group $Im\bar{3}m$ with phase angle $\alpha = 0$ according to the mean curvature calculated at the centre of mass of each tessellating polygon. Right: Colouring of the nodal surface approximation to the I-WP surface (Table 4).

Table 5
Summary of the results of surface approximation (bcc = body-centred, fcc = face centred)[a]

Surface	P	D	G	I-WP
Points per unit cell	2160	8640	2400	3120
Leading term	See Eq. (3a)	See Eq. (3b)	See Eq. (3c)	See Eq. (3d)
rms mean curvature of leading term/length^{-2}	3.2148×10^{-2}	3.4567×10^{-3}	1.0339×10^{-3}	0.1394
Number of terms fitted	5 and 2	3	15	8 + constant
Terms added	All	fcc	bcc	bcc
rms mean curvature of fitted surface/length^{-2}	3.3077×10^{-6} (5 terms) 1.6954×10^{-4} (2 terms)	1.3388×10^{-5}	3.03102×10^{-6}	2.62507×10^{-4}
rms error in $f(x,y,z) = 0$	2.1017×10^{-6} (5 terms) 4.7356×10^{-5} (2 terms)	1.2940×10^{-5}	5.72459×10^{-5}	1.57924×10^{-4}
Number of polygons used	11 396 (5 terms) 19 148 (2 terms)	18 122	14 613	8976
Exact normalised surface-to-volume ratio, $\mathscr{A}/\mathscr{V}^{2/3}$	2.345102 884	2.417652872	2.453680568	3.464101616
$\mathscr{A}/\mathscr{V}^{2/3}$ for the leading term	2.353 407	2.418401	2.453824	3.556094
$(\mathscr{A}/\mathscr{V}^{2/3})_{\text{leading}}/(\mathscr{A}/\mathscr{V}^{2/3})_{\text{exact}}$	1.003 541	1.000309	1.000058	1.026556
$(\mathscr{A}/\mathscr{V}^{2/3})_{\text{fitted}}$	2.345217 (5 terms) 2.345211 (2 terms)	2.418266	2.453681	3.464180
$(\mathscr{A}/\mathscr{V}^{2/3})_{\text{fitted}}/(\mathscr{A}/\mathscr{V}^{2/3})_{\text{exact}}$	1.004867 (5 terms) 1. 0000459 (2 terms)	1.000253	1.000000	1.000023

[a] $\mathscr{A}/\mathscr{V}^{2/3}$ (dimensionless), where $\mathscr{A}$ and $\mathscr{V}$ are the area and volume of the unit cell, respectively, is the normalized surface-to-volume ratio.

$h+k+l$ is even, i.e., {1 1 0}, {2 0 0}, {2 1 1}, {2 2 0}, etc. The D surface is face-centred cubic and requires only terms where the $\{hkl\}$ are all odd or all even. The P surface has a primitive cell, and all terms must be included. For the unbalanced I-WP surface a constant term, a_0, has been added to (7).

As more terms are added to the expansion, the quality of the nodal approximation greatly improves, but the values of the coefficients change, so that the basis set for expansion is non-orthogonal (Tables 1–4). The leading terms were given a weighting of 1. The colouring of the surfaces generated by the full nodal approximations is shown on the right-hand side of Figs. 1–4, and the numerical results are given in Table 5. It is clear that the P, D and G surfaces are approximated almost perfectly using PNS with 5, 3 and 15 Fourier terms. Using only two terms for the P surface gives only a slightly worse approximation (surface not shown).

Even with the constant term included, the nodal approximation for the I-WP surface is less satisfactory, and the colouring still reveals synclastic regions (Fig. 4). The values of all the coefficients in Table 4 are relatively large and do not decrease as more terms are added. This suggests that the expansion for this surface converges very slowly, and many more Fourier terms are required to achieve the same degree of accuracy as for the other surfaces.

The PNS are based on simple trigonometric functions, and provide a more readily accessible representation of TPMS than the analytical methods or the Enneper–Weierstrass parameterisation. The results enable the study of the mechanical properties of TPMS (vital for their use in engineering materials), the calculation of geodesic surface trajectories of molecules on the surface, and finally percolation and diffusion coefficients, needed to model the catalytic activity and related properties of curved objects.

References

[1] M.P. do Carmo, Differential Geometry of Curves and Surfaces, Prentice-Hall, Engelwood Cliffs, NJ, 1976.
[2] S. Hyde, S. Andersson, K. Larsson, Z. Blum, T. Landh, S. Lidin, B.W. Ninham, The Language of Shape, The Role of Curvature in Condensed Matter: Physics, Chemistry and Biology, Elsevier, Amsterdam, 1997.
[3] H.U. Nissen, Science 166 (1969) 1150.
[4] F.J. Almgren, Math. Intelligencer 4 (1982) 164.
[5] S. Andersson, S.T. Hyde, K. Larsson, S. Lidin, Chem. Rev. 88 (1988) 221.
[6] W. Longley, T.J. MacIntosh, Nature 303 (1983) 612.
[7] J.C.C. Nitsche, Lectures on Minimal Surfaces, vol. 1, Cambridge University Press, Cambridge, 1989.
[8] A. Fogden, J. de Physique (Paris) I 2 (1992) 233.
[9] A. Fogden, M. Haeberlein, S. Lidin, J. de Physique (Paris) I 3 (1993) 2371.
[10] A. Fogden, M. Haeberlein, J. Chem. Soc. Faraday Trans. 90 (1994) 263.
[11] D. Cvijović, J. Klinowski, J. de Physique (Paris) I 2 (1992) 2207.
[12] D. Cvijović, J. Klinowski, J. de Physique (Paris) I 2 (1992) 2191.
[13] D. Cvijović, J. Klinowski, J. de Physique (Paris) I 2 (1992) 137.
[14] P.J.F. Gandy, D. Cvijović, A.L. Mackay, J. Klinowski, Chem. Phys. Lett. 314 (1999) 543.
[15] P.J.F. Gandy, J. Klinowski, Chem. Phys. Lett. 321 (2000) 363.
[16] P.J.F. Gandy, J. Klinowski, Chem. Phys. Lett. 322 (2000) 579.
[17] D. Cvijović, J. Klinowski, Chem. Phys. Lett. 226 (1994) 93.
[18] H. Karcher, Manuscripta Mathematica 64 (1989) 291.
[19] K.A. Brakke, Exp. Math. 1 (1992) 141.
[20] M.R. Halse, Philos. Trans. Roy. Soc. London A 265 (1969) 507.
[21] H.G. von Schnering, R. Nesper, Z. Physik. B 83 (1991) 407.
[22] A.L. Mackay, Philos. Trans. Roy. Soc. London A 442 (1993) 47.
[23] J. Klinowski, A.L. Mackay, H. Terrones, Philos. Trans. Roy. Soc. London A 354 (1996) 1975.
[24] C.E. Weatherburn, The Differential Geometry of Three Dimensions, vol. II, Cambridge University Press, 1930, p. 85.
[25] I.S. Barnes, S.T. Hyde, B.W. Ninham, J. de Physique (Paris) C 51 (1990) 7.
[26] A.L. Mackay, Chem. Phys. Lett. 221 (1994) 317.
[27] I. Barnes, Aust. Math. Soc. Gazette 17 (1990) 99.
[28] C.A. Lambert, L.H. Radzilowski, E.L. Thomas, Philos. Trans. Roy. Soc. London A 354 (1996) 2009.
[29] S. Brenner, L.B. McCusker, C. Bärlocher, J. Appl. Crystallogr. 30 (1997) 1167.
[30] S. Wolfram, Mathematica: a System for Doing Mathematics by Computer, 2nd ed., Addison-Wesley, Redwood City, 1991.
[31] K. Lonsdale, N.F.M. Henry (Eds.), International Tables for X-ray Crystallography, vol. 1, Kynoch Press for the International Union of Crystallography, Birmingham, 1952.

[32] K. Lonsdale, W.T. Astbury, Philos. Trans. Roy. Soc. London A 224 (1924) 221.
[33] K. Lonsdale, Structure Factor Formulae for the 230 Space Groups, International Tables for the Determination of Crystal Structures, Bornträger, Berlin, 1935.
[34] K. Lonsdale, Simplified Structure Factor and Electron Density Formulae for the 230 Space Groups of Mathematical Crystallography, Bell for the Royal Institution, London, 1936, p. 181.
[35] W.H. Press, B.P. Flannery, S.A. Teukolsky, W.T. Vetterling, Numerical Recipes, Cambridge University Press, Cambridge, UK, 1986.